



Live-Bed Local Pier Scour Experiments

D. Max Sheppard, M.ASCE¹; and William Miller Jr.²

Abstract: Local clear-water and live-bed scour tests were performed for a range of water depths and flow velocities with two different uniform cohesionless sediment diameters (0.27 and 0.84 mm) and a circular pile with a diameter of 0.15 m. The tests were performed in a tilting flume (1.5 m wide, 1.2 m deep, and 45 m long) located in the Hydraulics Laboratory at the University of Auckland in Auckland, New Zealand. These tests extend local scour data obtained in controlled experiments to velocity ratio (V/V_c) values as high as 6. This is near the velocity where the peak live-bed scour occurs for the sediment and flow conditions. Scour depth predictions are made with four different local scour equations for the conditions of the tests and the results compared with the measured values.

DOI: 10.1061/(ASCE)0733-9429(2006)132:7(635)

CE Database subject headings: Scour; Experimentation; Piers; Piles; Bridge foundation; Erosion; Bedforms.

Introduction

Local sediment scour tests in the live-bed scour range of velocities are, in general, difficult to perform and the results difficult to analyze due to the presence of bed forms. This paper presents the results of 24 local sediment scour experiments conducted by the lead writer in the Hydraulics Laboratory at the University of Auckland in Auckland, New Zealand. The tests were performed with a single circular pile, two uniform diameter cohesionless sediments, and a range of water depths and flow velocities. All but four of the tests were conducted in the live-bed scour range (i.e., the flow velocities were greater than that required to initiate sediment movement upstream of the pile). The scour depth results for all of the tests and representative time history plots of the scour depths are presented in this paper. The reader is referred to the technical report by Sheppard (2003a) for additional data and details of the analyses. In addition, four different commonly used local scour prediction equations are evaluated for the conditions of the experiments and the results compared with the measured data.

Live-Bed Local Scour Tests

Live-bed local sediment scour tests were performed on a circular pile with a diameter of 0.152 m and sediments with median grain sizes of 0.27 and 0.84 mm. The sediment size distributions were near uniform with standard deviations ($\sigma = \sqrt{D_{84}/D_{16}}$) of 1.33 for the 0.27 mm sediment and 1.32 for the 0.84 mm sediment.

Experimental Facilities

A plan drawing of the flume used for these experiments is shown in Fig. 1. All of the tests were conducted in this tilting flume which is 1.5 m wide, 1.2 m deep, and 45 m long. The flume is located in the Hydraulics Laboratory in the Civil and Environmental Engineering Department at the University of Auckland in Auckland, New Zealand. It has two pumps for recirculating the water with a combined capacity of 1.2 m³/s and a sediment pump with adequate capacity. The bed load sediment (sediment moving along the bed) is trapped and pumped to the flume entrance with the sediment pump. Suspended sediment is pumped with the water to the entrance with either or both of the water pumps.

Instrumentation

The instrumentation used in this research measured the flow parameters and scour depth. The flow parameters monitored were flow discharge (indirectly), velocity at specific locations, water depth, and temperature. The scour depth was monitored with internal video cameras and arrays of acoustic transponders. The bed and water elevations at the walls on both sides of the flume were monitored with externally mounted cameras for most of the live-bed tests.

Two miniature video cameras were mounted on a traversing mechanism located inside the pile. Three arrays of high frequency acoustic transponders were attached to the cylinder just below the water surface to measure bed elevations at 12 locations in the scour hole at specified time intervals throughout the experiment. Each array contained four crystals, which produced a 2.5 cm diameter acoustic beam at the transducer. The spread angle of the beam was approximately 1.5° and the footprint of the beam (area of the acoustic beam at the bed) varied with the water and scour hole depths. The time required for the acoustic pulse to travel to the bed and return to the transponder was measured and the distance from the transponder to the bed was computed based on the speed of sound in water at that temperature. A schematic diagram and photograph of this instrument array are given in Figs. 2 and 3.

Prior to starting the tests, numerous vertical velocity profiles were measured and integrated to determine the flow discharge as a function of pump rpm (which can be precisely controlled). The

¹Professor of Civil and Coastal Engineering, Univ. of Florida, Gainesville, FL 32611. E-mail: sheppard@ufl.edu

²Project Engineer, Taylor Engineering, Inc., 9000 Cypress Green Dr., Jacksonville, FL 32256. E-mail: wmiller@taylorentengineering.com

Note. Discussion open until December 1, 2006. Separate discussions must be submitted for individual papers. To extend the closing date by one month, a written request must be filed with the ASCE Managing Editor. The manuscript for this paper was submitted for review and possible publication on March 10, 2004; approved on August 19, 2005. This paper is part of the *Journal of Hydraulic Engineering*, Vol. 132, No. 7, July 1, 2006. ©ASCE, ISSN 0733-9429/2006/7-635-642/\$25.00.

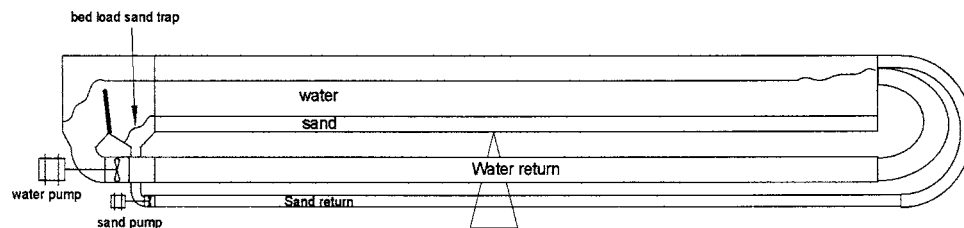


Fig. 1. Schematic drawing of the flume

velocity measurements were made with an acoustic Doppler velocimeter (ADV). During the tests, the sectionally averaged velocity was determined from the pump rpm and the water depth at the section. The water depth at the test section was measured using scales attached to the glass walls of the flume and the water temperature measured with a glass thermometer.

Experimental Procedure

In order to insure repeatability and to isolate the effects of various parameters on equilibrium scour depth and rate of scour, a strict procedure was followed throughout these tests. A summary of the experimental procedure used is outlined below. The procedure is divided into the tasks performed before, during, and after the experimental run.

Pre-experiment:

1. Compact and level the bed in the flume;
2. Fill the flume slowly and allow standing until the air trapped in the sediment has escaped;
3. Take pre-experiment photographs; and
4. Check all instrumentation.

During experiment:

1. Measure the scour depth as a function of time with acoustic transponders and video cameras;
2. Measure the velocity, water depth, and temperature;
3. Monitor bed elevation at flume walls in test section with external video cameras; and
4. Monitor bed forms during live-bed tests.

Post-experiment:

1. Take post-experiment photographs;
2. Observe and note bed condition throughout the flume (presence of bed forms, etc.);

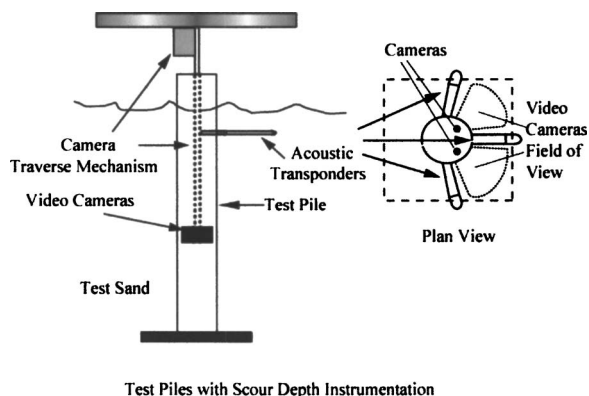


Fig. 2. Local scour depth measuring instruments

3. Survey the scour hole with a point gauge; and
4. Reduce and analyze the data.

Experimental Results

A significant quantity of local sediment scour data and bed form information were gathered during this research program. Even though most of the tests were performed in the live-bed scour range a few tests were conducted in the clear-water scour range to fill in gaps in the existing data set. The structure, sediment, and flow conditions under which the tests were conducted are summarized in Table 1. Column 9 in Table 1 (labeled "T") is the duration of the test in minutes. The scour depth data are given in Table 2. All of the experiments conducted as part of this work were relatively long in duration, for live-bed scour tests, and thus the scour depths were at or very near equilibrium at the end of the test. Large bed forms migrated through the scour hole during a number of the live-bed scour tests as can be seen in Figs. 3–5. Curves were fit to the data (Figs. 4 and 5) so that local scour depths could be extracted from the total scour which included bed forms. Column 6 in Table 2 lists the values of the fit curves at the end of the test. Column 7 in Table 2 is the equilibrium scour depths obtained by setting time equal to infinity in the curve fit equations. Values of equilibrium scour depth for the clear-water scour tests are thought to be conservative due to the properties of the fit curves and the extrapolation method. That is, the equilibrium values in the table for the clear-water tests are thought to be higher than what have been measured had the test lasted until scour ceased.

Discussion of Results

Two different mathematical functions were used to fit the local scour time history data. These functions are



Fig. 3. Scour hole after live-bed scour test with large bed forms

Table 1. Structure, Sediment, and Flow Test Conditions

Test	D (m)	D_{50} (mm)	Θ (degrees)	y_0 (m)	V (m/s)	V_c (m/s)	V_{lp} (m/s)	T (min)
1	0.152	0.27	25	0.42	0.17	0.27	1.61	1,740
2	0.152	0.27	22	0.42	0.62	0.28	1.62	307
3	0.152	0.27	24	0.43	0.88	0.28	1.63	442
4	0.152	0.27	23	0.4	1.1	0.28	1.58	465
5A	0.152	0.27	23	0.4	1.26	0.28	1.58	257
5B	0.152	0.27	24	0.4	1.43	0.27	1.58	94
6	0.152	0.27	24	0.4	1.64	0.27	1.58	104
7A	0.152	0.27	24	0.2	0.55	0.25	1.25	103
7B	0.152	0.27	24	0.2	0.72	0.25	1.25	67
8	0.152	0.27	23	0.43	0.69	0.28	1.63	1,470
9	0.152	0.27	23	0.49	0.25	0.28	1.75	2,760
10	0.152	0.84	23	0.43	0.37	0.41	1.88	1,130
11	0.152	0.84	25	0.38	0.58	0.41	1.86	3,053
12	0.152	0.84	25	0.38	0.74	0.41	1.86	1,019
13	0.152	0.84	26	0.38	1.05	0.41	1.87	966
14	0.152	0.84	23	0.38	1.21	0.41	1.86	101
15	0.152	0.84	26	0.38	1.37	0.41	1.87	60
16	0.152	0.84	26	0.38	1.52	0.41	1.87	60
17	0.152	0.84	23	0.3	1.52	0.4	1.79	65
18	0.152	0.84	23	0.3	1.76	0.4	1.79	75
19	0.152	0.84	24	0.3	1.85	0.4	1.8	30
20	0.152	0.84	24	0.3	1.99	0.4	1.8	20
21	0.152	0.84	24	0.3	2.16	0.4	1.8	20
22	0.152	0.84	18	0.43	0.25	0.41	1.87	19,920

Table 2. Nondimensional Parameters, Measured and Equilibrium Scour Depths

Test	y_0/D	V/V_c	D/D_{50}	V_{lp}/V_c	Measured d_s (m)	d_{se} (m)	d_{se}/D
1	2.76	0.63	563	5.96	0.11	0.13	0.86
2	2.76	2.21	563	5.79	0.24 ^a	0.22	1.45
3	2.83	3.14	563	5.82	0.34 ^a	0.24	1.58
4	2.63	3.93	563	5.64	0.26 ^a	0.25	1.64
5A	2.63	4.50	563	5.64	0.30 ^a	0.27	1.78
5B	2.63	5.30	563	5.85	0.29 ^a	0.27	1.78
6	2.63	6.07	563	5.85	0.32 ^a	0.30	1.97
7A	1.32	2.20	563	5.00	0.18	0.18	1.18
7B	1.32	2.88	563	5.00	0.24 ^a	0.22	1.45
8	2.83	2.46	563	5.82	0.33 ^a	0.23	1.51
9	3.22	0.89	563	6.25	0.14	0.15	0.99
10	2.83	0.90	181	4.59	0.20	0.24	1.58
11	2.50	1.41	181	4.54	0.19 ^a	0.17	1.12
12	2.50	1.80	181	4.54	0.27 ^a	0.25	1.64
13	2.50	2.56	181	4.56	0.29 ^a	0.25	1.64
14	2.50	2.95	181	4.54	0.29 ^a	0.23	1.51
15	2.50	3.34	181	4.56	0.29 ^a	0.25	1.64
16	2.50	3.71	181	4.56	0.31	0.26	1.71
17	1.97	3.80	181	4.48	0.31 ^a	0.26	1.71
18	1.97	4.40	181	4.48	0.30 ^a	0.26	1.71
19	1.97	4.63	181	4.50	0.28 ^a	0.27	1.78
20	1.97	4.98	181	4.50	0.32 ^a	0.28	1.84
21	1.97	5.40	181	4.50	0.34 ^a	0.30	1.97
22	2.83	0.61	181	4.56	0.16	0.20	1.32

^aMeasured values at the end of the test with bed forms removed.

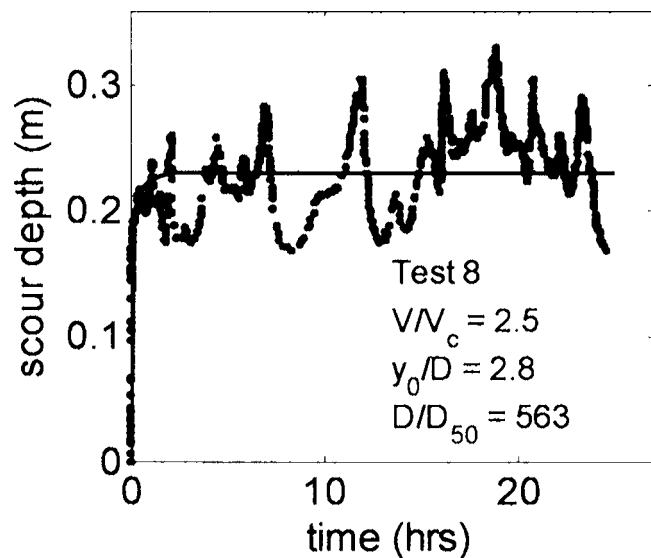


Fig. 4. Time history plot with fit curve of Test 8

$$d_s(t) = a \left[1 - \frac{1}{(1 + abt)} \right] + c \left[1 - \frac{1}{(1 + cdt)} \right] \quad (1)$$

and

$$d_s(t) = a[1 - \exp(-bt)] + c[1 - \exp(-dt)] \quad (2)$$

The equation that produced the best least-squares fit to the data was used to obtain the equilibrium scour depths for the tests. Once the coefficients in Eqs. (1) or (2) were determined, time was set equal to infinity to obtain the equilibrium depth. In order to produce accurate estimates of equilibrium scour depths, the writers have found that the duration of the test must be at least that recommended by Melville [i.e., the rate of scour should be less than 5% of pile diameter in a 24 h period; Melville and Chiew (1999)]. Figs. 4 and 5 are plots of typical scour depth time histories with the associated fit equations. Bed form migration through the scour hole is clearly visible in the data.

Many of the live-bed tests reached equilibrium so quickly that little experimental data was available at scour depths less than

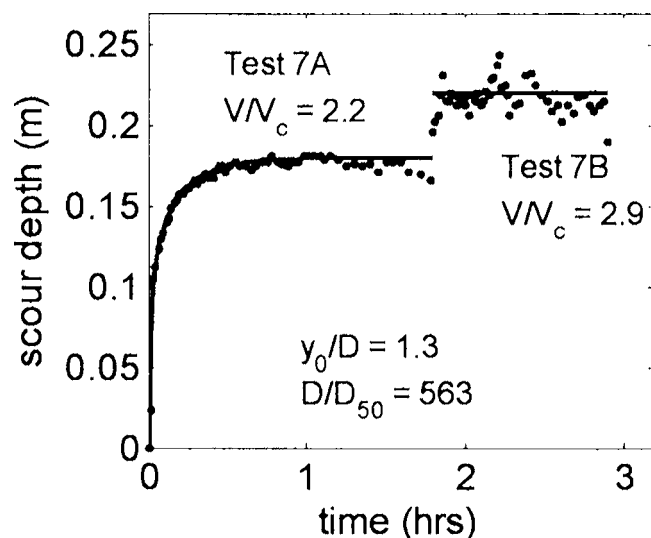


Fig. 5. Time history plot with fit curve of Tests 7A and 7B

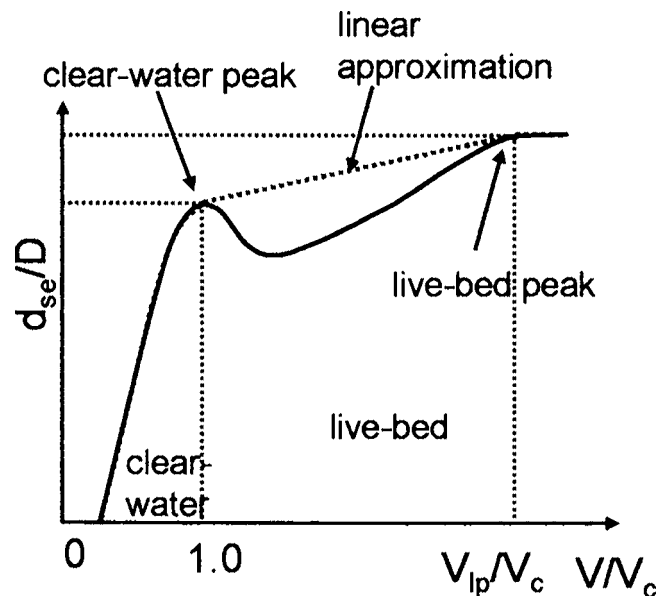


Fig. 6. Normalized scour depth (d_{se}/D) versus flow intensity (V/V_c)

equilibrium. To optimize the amount of data obtained for the available time (by reducing the required setup time), some of the tests were a continuation of a previous test (e.g., Test 7B in Fig. 5) where the flow velocity was increased at the end of a test and a second equilibrium depth obtained at a higher velocity ratio. Table 2 lists the equilibrium scour depths (d_{se}) in Column 7.

The solid line in the schematic diagram in Fig. 6 illustrates the behavior of the normalized scour depth (d_{se}/D) as a function of flow intensity (V/V_c) as determined by several researchers (Ettema 1980; Chiew 1984; Melville and Chiew 1999; Sheppard et al. 1995; Sheppard 1999). It shows a peak in the equilibrium scour depth at the transition from clear-water to live-bed conditions, a decrease in equilibrium scour depth just beyond this peak, and a second peak in the live-bed scour range (believed to occur where the bed "planes out"). The velocity at the second peak is referred to here as the "live-bed peak velocity" and is denoted by V_{lp} . From van Rijn (1993, pp. 5.3 and 5.4), the bed "planes out" when the depth Froude number ($F = V/\sqrt{gy_0}$) exceeds 0.8 and the sediment transport parameter $[(\tau_b - \tau_c)/\tau_c]$ exceeds 25. Therefore, the live-bed peak velocity can be determined by calculating the depth averaged velocity which satisfies both conditions. Table 1, Column 8 lists this velocity for each test.

Table 2 lists the nondimensional parameters (y_0/D^* , V/V_c , D^*/D_{50} , V_{lp}/V_c) which are needed for Sheppard's local scour equations (Sheppard 2003a). Sheppard defines D^* as the effective circular pile diameter and d_{se}/D^* as the normalized equilibrium scour depth. In other words, if the pile has some shape other than circular, D^* is the diameter of a circular pile that will experience the same equilibrium scour depth for the same flow and sediment conditions. Since the pile for the tests presented here was circular, $D^* = D$.

Sheppard's equations are given below.

In the *clear-water scour range* ($0.47 \leq V/V_c \leq 1$)

$$\frac{d_{se}}{D^*} = 2.5f_1\left(\frac{y_0}{D^*}\right)f_2\left(\frac{D^*}{D_{50}}\right)\left\{1 - 1.75\left[\ln\left(\frac{V}{V_c}\right)\right]^2\right\} \quad (3)$$

In the *live-bed scour range up to the live-bed peak* ($1 < V/V_c \leq V_{lp}/V_c$)

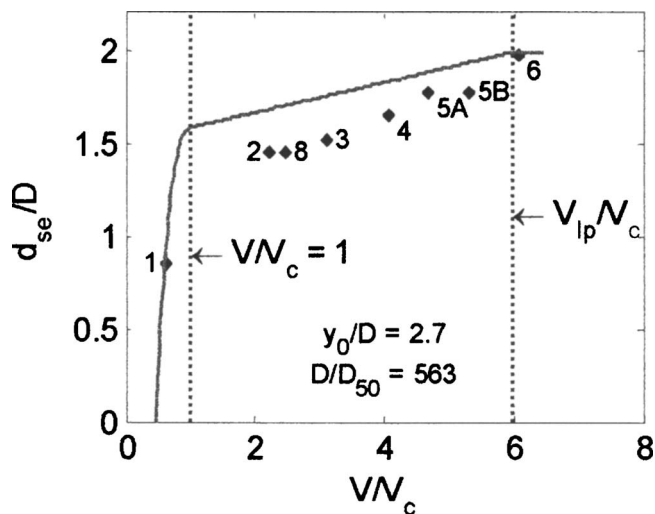


Fig. 7. Measured and predicted d_{se}/D versus V/V_c for Tests 1–4, 5A, 5B, 6, and 8

$$\frac{d_{se}}{D^*} = f_1\left(\frac{y_0}{D^*}\right) \left[2.2 \left(\frac{V/V_c - 1}{V_{lp}/V_c - 1} \right) + 2.5 f_2\left(\frac{D^*}{D_{50}}\right) \left(\frac{V_{lp}/V_c - V/V_c}{V_{lp}/V_c - 1} \right) \right] \quad (4)$$

and in the *live-bed scour range above the live-bed peak* ($V/V_c > V_{lp}/V_c$)

$$\frac{d_{se}}{D^*} = 2.2 f_1\left(\frac{y_0}{D^*}\right) \quad (5)$$

where

$$f_1\left(\frac{y_0}{D^*}\right) = \tanh\left[\left(\frac{y_0}{D^*}\right)^{0.4}\right] \quad (6)$$

and

$$f_2\left(\frac{D^*}{D_{50}}\right) = \frac{D^*/D_{50}}{0.4(D^*/D_{50})^{1.2} + 10.6(D^*/D_{50})^{-0.13}} \quad (7)$$

One of the objectives of the experiments presented here was to provide data for evaluating Sheppard's equations in the live-bed scour range of velocities. For the purpose of this evaluation, the tests were divided into groups that had equal or nearly equal values of D/D_{50} and y_0/D . Comparisons between the predicted [using Eqs. (3)–(7)] and the measured values of normalized equilibrium scour depths are given in Figs. 7–10. The solid lines in these figures are plots of Eqs. (3)–(7) evaluated at the specified constant values of D/D_{50} and y_0/D for the complete range of V/V_c . As expected, Sheppard's equations overpredict the scour depths in all cases but one.

Three additional commonly used scour prediction equations were also evaluated for the conditions of the experiments. The Colorado State University (or HEC-18) equation (Richardson and Davis 2001) is

$$\frac{d_{se}}{D} = 2.0 K_3 \left(\frac{y_0}{D} \right)^{0.35} F^{0.43} \quad (8)$$

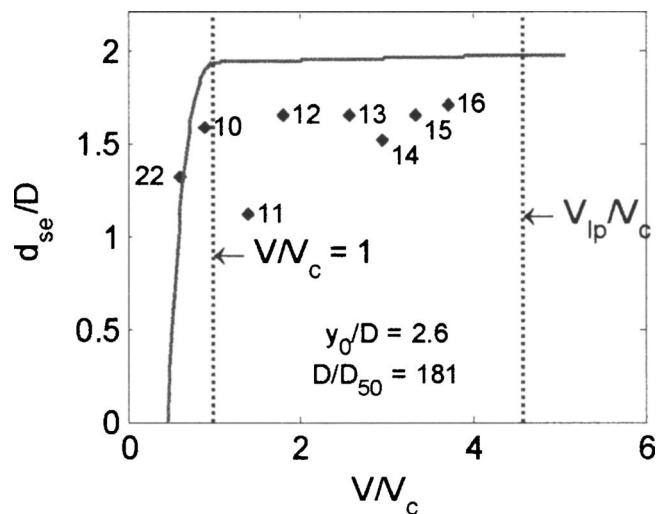


Fig. 8. Measured and predicted d_{se}/D versus V/V_c for Tests 10–16 and 22

where K_3 accounts for bed forms (K_3 is 1.1 for plane bed and small dunes, 1.1 to 1.2 for medium dunes, and 1.3 for large dunes). The maximum value for d_{se}/D is capped at 2.4 for $F \leq 0.8$, and at 3.0 for $F > 0.8$.

Melville's equation (Melville 1997) is a function of V/V_c , D/D_{50} , and y_0/D . For a circular pile and uniform sediment, Melville's equation is

$$\frac{d_{se}}{D} = K_I K_d K_{yD} \quad (9)$$

where $K_I = V/V_c$ if $V/V_c < 1$ and $K_I = 1$ otherwise, $K_d = 0.57 \log(2.24 D/D_{50})$ if $D/D_{50} \leq 25$ and $K_d = 1$ otherwise, and $K_{yD} = 2.4$ if $D/y_0 < 0.7$, $K_{yD} = 2\sqrt{y_0/D}$ if $0.7 \leq D/y_0 \leq 5$, and $K_{yD} = 4.5 y_0/D$ if $D/y_0 > 5$.

Finally, Breusers et al. (1977) presented an equation that was a function of V/V_c and y_0/D only. For circular piers, the equation is

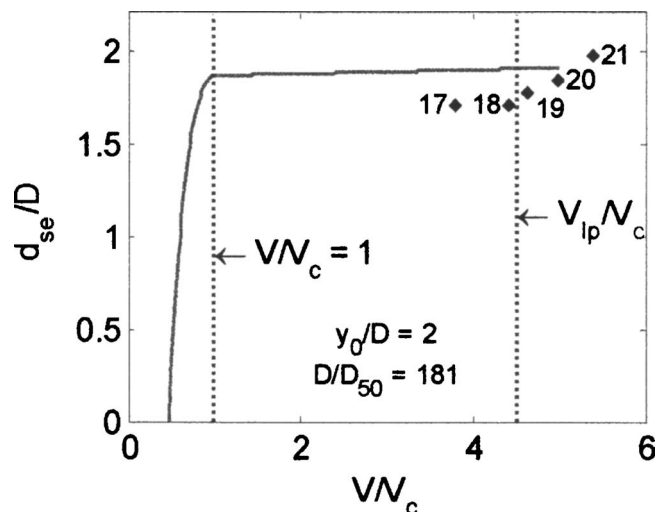


Fig. 9. Measured and predicted d_{se}/D versus V/V_c for Tests 17–21

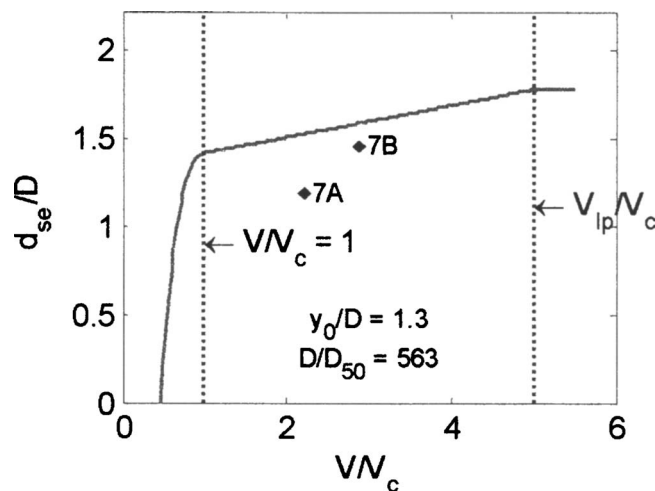


Fig. 10. Measured and predicted d_{se}/D versus V/V_c for Tests 7A and 7B

$$\frac{d_{se}}{D} = K_v \tanh\left(\frac{y_0}{D}\right) \quad (10)$$

where $K_v=0$ for $V/V_c \leq 0.5$, $K_v=2(V/V_c)-1$ for $0.5 < V/V_c \leq 1$, and $K_v=1$ for $V/V_c > 1$.

Eqs. (8)–(10) and Sheppard's equations [Eqs. (3)–(7)] were used to predict the normalized equilibrium scour depth for the test conditions in Table 1. Table 3 lists the measured and computed values for each test. Figs. 11 and 12 present the difference be-

Table 3. Measured and Predicted Scour Comparison

	Test	Measured	d_{se}/D			
			UF	CSU	Melville	Breusers
Fig. 11	1	0.86	0.99	1.08	1.51	0.52
	7A	1.18	1.52	1.47	2.30	1.73
	2	1.45	1.69	1.71	2.40	1.98
	8	1.51	1.71	1.80	2.40	1.99
	7B	1.45	1.58	1.66	2.30	1.73
	3	1.58	1.77	2.00	2.40	1.99
	4	1.64	1.83	2.18	2.40	1.98
	5A	1.78	1.88	2.31	2.40	1.98
	5B	1.78	1.93	2.40	2.40	1.98
	6	1.97	1.98	2.85	2.40	1.98
Fig. 12	22	1.32	1.12	1.28	1.46	0.44
	10	1.58	1.92	1.52	2.16	1.59
	11	1.12	1.93	1.64	2.40	1.97
	12	1.64	1.93	1.82	2.40	1.97
	13	1.64	1.94	2.12	2.40	1.97
	14	1.51	1.95	2.25	2.40	1.97
	15	1.64	1.95	2.38	2.40	1.97
	16	1.71	1.96	2.40	2.40	1.97
	17	1.71	1.89	2.41	2.40	1.92
	18	1.71	1.90	2.56	2.40	1.92
	19	1.78	1.90	2.88	2.40	1.92
	20	1.84	1.90	2.97	2.40	1.92
	21	1.97	1.90	3.00	2.40	1.92

tween the computed and measured values as a percentage of the experimental value

$$\% \text{ difference} = \left(\frac{\text{computed} - \text{measured}}{\text{measured}} \right) \times 100\% \quad (11)$$

Both Table 3 and Figs. 11 and 12 list the tests in order of increasing V/V_c . Fig. 11 shows the results for $D/D_{50}=563$ and Fig. 12 shows the results for $D/D_{50}=181$.

All four equations overpredict the experimental values for most of the tests. In some cases the overprediction is significant (in excess of 100% in one case). The average and standard deviations (respectively) of the percentage differences for the four equations are Sheppard (16.6 and 18.2%), CSU (33.1 and 17.5%), Melville (51.7 and 26.9%), and Breusers (16.1 and 28.6%). The differences between the predictions by the four equations will be even greater for larger structures due to the differences in the D/D_{50} terms in the equations. For example, equilibrium scour depth predictions by Sheppard, CSU, Melville, and Breusers for a 15 m diameter circular structure in cohesionless sediment with a $D_{50}=0.3$ mm subjected to a flow with a water depth of 5 m, a depth-averaged velocity of 2.0 m/s, and a temperature of 18°C are 10.0, 12.6, 18.8, and 5.6 m, respectively (not including bed-forms).

Summary and Conclusions

The experiments in this study have extended the live-bed local scour depth data set. These live-bed data are consistent with data obtained by Ettema (1980) and Chiew (1984) in showing the decreased dependence of normalized equilibrium scour on D/D_{50} at higher values of V/V_c . A possible explanation as to why there is a scour depth dependence on D/D_{50} and why this dependence decreases with increased values of this parameter was given by Sheppard (2004).

Sheppard's equations, which have already been tested for large (up to 0.914 m diameter) structures in the clear-water scour range (Sheppard 2003b) yield good results in the live-bed scour range covered by these experiments. The comparisons between several commonly used local scour equations and the measured data are made and Sheppard's equations appear to perform well for the range of conditions covered by the experiments.

It should be noted that bedform wave amplitudes should be estimated using one of the predictive equations in the literature and this value along with the other scour components (contraction, aggradation/degradation, effects of lateral stream migration) should be added to the predicted local scour depth to obtain the total scour depth at the structure.

Acknowledgments

The writers thank Rick Renna, Shawn McLemore, and Richard Long with the Florida Department of Transportation for their technical input to and financial support of this research. Thanks also go to Electronics Engineer Sidney Schofield, technicians Jim Joiner and Chuck Broward, and machinist Vernon Sparkman for assisting with the design and construction of the instrumentation. Very special thanks to Dr. Bruce Melville and his staff, Jim Beckner and Raymond Hoffmann, for their assistance with the construction of the test structures, flume modifications, and the conduct of the experiments. The writers are indebted to Univer-

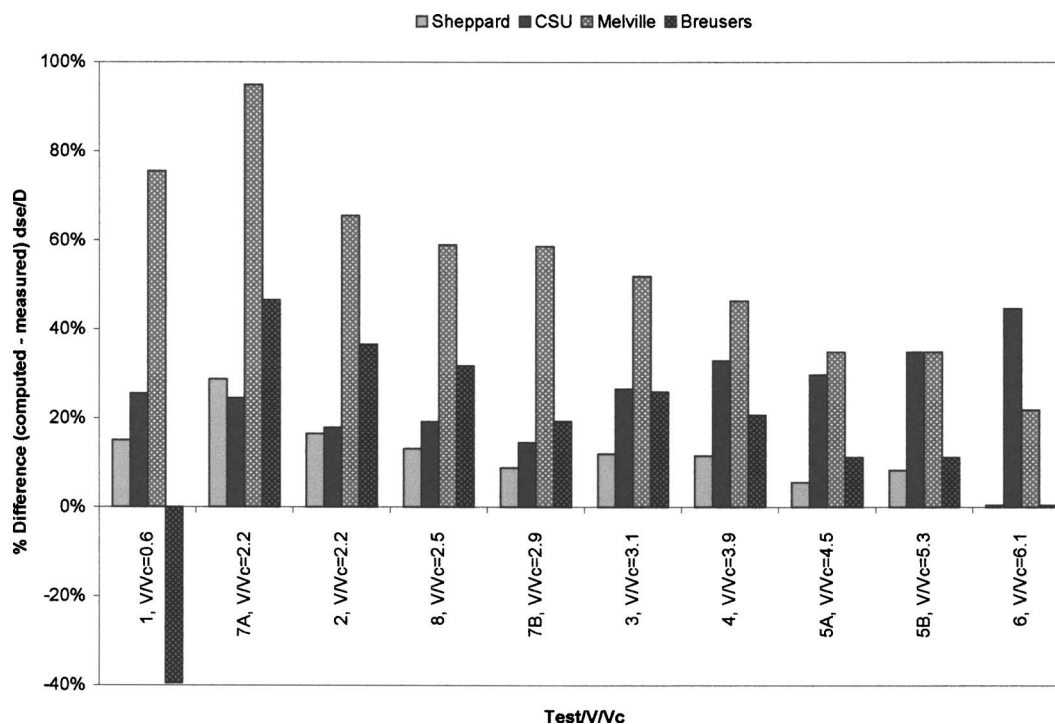


Fig. 11. Percent difference in computed and measured d_{se}/D for Tests 1–8 ($D/D_{50}=563$)

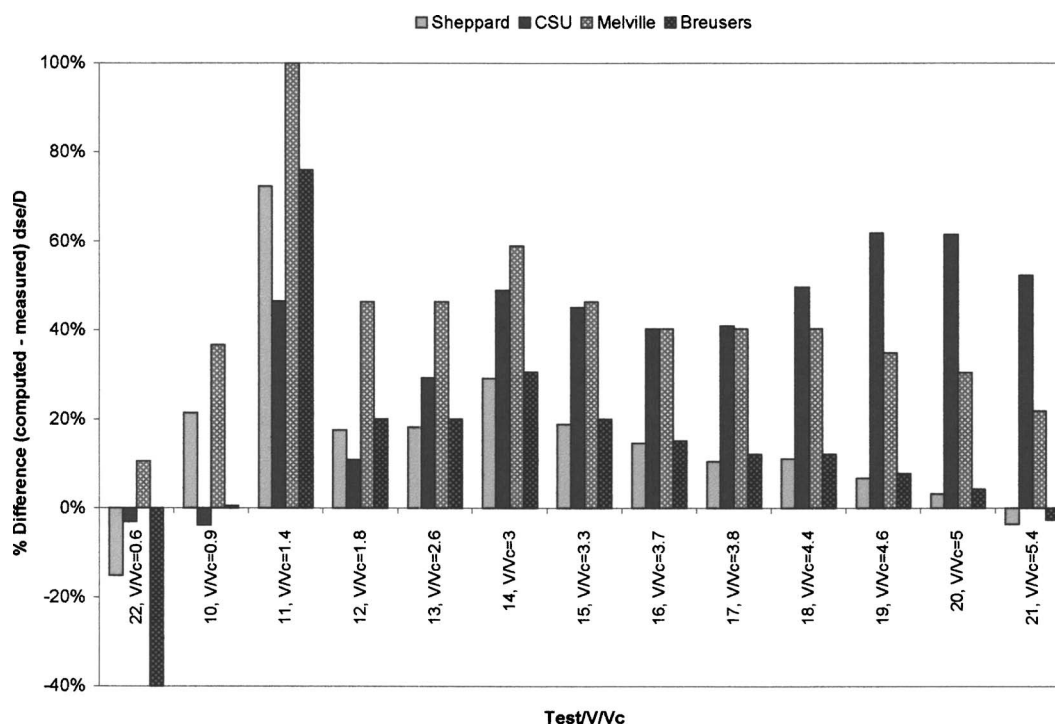


Fig. 12. Percent difference in computed and measured d_{se}/D for Tests 10–22 ($D/D_{50}=181$)

sity of Auckland graduate students Sjoerd van Ballegooy and Thomas Macdougall Clunie for their diligent and dedicated work in running the tests.

Notation

The following symbols are used in this paper:

- a, b, c, d = coefficients in curve fit equations;
- D = circular pile diameter;
- D^* = effective structure width/diameter = $K_s D$;
- D_{16} = sediment size for which 16% of bed material is finer;
- D_{50} = median sediment grain diameter;
- D_{84} = sediment size for which 84% of bed material is finer;
- d_s = scour depth at end of experiment;
- $d_s(t)$ = scour depth as function of time;
- d_{se} = equilibrium scour depth;
- F = Froude number, $F = V / \sqrt{gy_0}$;
- g = acceleration of gravity;
- T = test duration;
- t = time;
- V = depth averaged velocity;
- V_c = averaged velocity at threshold condition for sediment motion (sediment critical velocity);
- V_{lp} = live-bed peak scour velocity (velocity where the bed planes out);
- y_0 = approach water depth;
- Θ = water temperature;
- σ = standard deviation of sediment particle size distribution, $\sqrt{D_{84}/D_{16}}$;
- τ_b = bed shear stress; and
- τ_c = critical bed shear stress.

References

- Breusers, H. N. C., Nicollet, G., and Shen, H. W. (1977). "Local scour around cylindrical piers." *J. Hydraul. Res.*, 15(3), 211–252.
- Chiew, Y. M. (1984). "Local scour at bridge piers." *Rep. No. 355*, Dept. of Civil Engineering, Univ. of Auckland, Auckland, New Zealand.
- Ettema, R. (1980). "Scour at bridge piers." *Rep. No. 236*, Dept. of Civil Engineering, Univ. of Auckland, Auckland, New Zealand.
- Melville, B. W. (1997). "Pier and abutment scour: Integrated approach." *J. Hydraul. Eng.*, 123(2), 125–136.
- Melville, B. W., and Chiew, Y. M. (1999). "Time scale for local scour at bridge piers." *J. Hydraul. Eng.*, 125(1), 59–65.
- Richardson, E. V., and Davis, S. R. (2001). "Evaluating scour at bridges." *Publication No. FHWA NHI 01-001, Hydraulic Engineering Circular No. 18*, Federal Highway Administration, U.S. Dept. of Transportation, Washington, D.C.
- Sheppard, D. M. (1999). "Conditions of maximum local structure-induced sediment scour." *Stream Stability and Scour at Highway Bridges, Compendium of Papers, Water Resources Engineering Conf. 1991 to 1998*, Everett V. Richardson and Peter F. Lagasse, eds., ASCE, Reston, Va.
- Sheppard, D. M. (2003a). "Large-scale and live-bed local pier scour experiments." *Coastal Engineering Technical Rep. No. 133*, Civil and Coastal Engineering Dept., Univ. of Florida, Gainesville, Fla.
- Sheppard, D. M. (2003b). "Large-scale clear-water local pier scour experiments." *Coastal Engineering Technical Rep. No. 131*, Civil and Coastal Engineering Dept., Univ. of Florida, Gainesville, Fla.
- Sheppard, D. M. (2004). "An overlooked local sediment scour mechanism." *Transportation Research Record. 1890*, Transportation Research Board, Washington, D.C., 107–111.
- Sheppard, D. M., Ontowirjo, B., and Zhao, G. (1995). "Local scour near single piles in steady currents." *Proc., 1st Hydraulics Engineering Conf.*, San Antonio, Tex.
- van Rijn, Leo C. (1993). *Principals of sediment transport in rivers, estuaries and coastal seas*, Aqua, Amsterdam, The Netherlands.